

# Ground states in a quasi-one-dimensional triangular Hubbard model

W. Z. Wang\*

*Department of Physics, Wuhan University, Wuhan 430072, People's Republic of China*

(Received 7 December 2004; revised manuscript received 1 June 2005; published 20 September 2005)

We study the ground state in a quasi-one-dimensional triangular Hubbard model using the exact numerical diagonalization, the constrained-path Monte Carlo, and the cluster perturbation theory. As the frustration hopping  $t$  is small the system exhibits short-range antiferromagnetic correlation. As  $t$  is greater than a critical point  $t_c$ , there is a transition from an antiferromagnetic state to a frustrated state, which is accompanied by a jump of local entanglement and an abrupt change of spin correlation. As  $t$  is greater than another critical point  $t_{c'}$ , the insulator-metal transition takes place. The successive order of two transitions depends on the on-site Coulomb interaction. The calculated spectra indicates that the spin-charge separation is destroyed by the frustration hopping. The frustrated state corresponds to the appearance of an additional dispersion band near the Fermi surface.

DOI: [10.1103/PhysRevB.72.125116](https://doi.org/10.1103/PhysRevB.72.125116)

PACS number(s): 71.27.+a, 75.30.Fv, 71.10.Fd

## I. INTRODUCTION

Geometrical frustration in strongly correlated electron systems has attracted a great deal of interest over the past decades.<sup>1-6</sup> In localized spin systems, magnetic frustration suppresses long-range order and stabilizes some exotic states such as the spin liquid resonating valence bond state or the valence bond crystal.<sup>7-9</sup> For example, due to the competition between the nearest exchange and the next-nearest exchange, the inorganic spin-Peierls compound  $\text{CuGeO}_3$  exhibits a transition from a gapless phase to a gapped dimerized ground state.<sup>10,11</sup> For an antiferromagnetic Heisenberg model on the pyrochlore lattice, when the ratio of the two competing exchange couplings is varied, quantum phase transitions occur between spin gap phases and the antiferromagnetic phases.<sup>12</sup> In itinerant systems, the interplay between geometrical frustration and strong electron correlation results in a complicated phase diagram containing many interesting phases. The 2D and 3D pyrochlore Hubbard models at the half filling show the transition from semimetal to spin-gapped insulator.<sup>13,14</sup> Frustration also assists the formation of Fermi quasiparticles by effectively suppressing the antiferromagnetic fluctuations.<sup>15,16</sup> For the half-filled Hubbard chain, frustration induces several phases: spin gapped metallic phase, disorder magnetic insulation phase, and Heisenberg insulator.<sup>17</sup>

The two-dimensional triangular lattice is a typical nonbipartite and frustrated lattice. In the triangular Heisenberg model, the existence of long-range Neel order is confirmed by quantum Monte Carlo techniques and exact diagonalization (ED).<sup>18</sup> The Hartree-Fock mean-field theory of the Hubbard model on isotropic triangular lattice<sup>19</sup> exhibits that with increasing the interaction strength  $U$ , there are four phases: paramagnetic metal, spiral metal, semimetallic linear spin-density wave, and an antiferromagnetic insulator. However, the ED result just indicates a transition between a paramagnetic metal and an antiferromagnetic insulator.<sup>20</sup> Recently, frustrated Hubbard ladders also have been studied.<sup>21</sup> Half-filled two-leg Hubbard ladders have spin-gapped short-range antiferromagnetic correlations while three-leg ladders have no gap and power law antiferromagnetic correlations.<sup>22</sup> For

half-filled frustrated Hubbard ladders, varying the degree of frustration can drive them across an insulator-metal transition.<sup>21</sup> Motivated by these developments, in this paper, we investigate the coupled Hubbard chains shown in Fig. 1. For the interchain coupling  $t=0$ , the system is decoupled to three isolated Hubbard chains. At half filling the physics is dominated by an antiferromagnetic insulating phase for all on site Hubbard repulsion  $U>0$ . The low-energy excitation spectra can be explained by underlying spinon and holon excitations.<sup>23</sup> However, if  $t$  is turned on, the system is frustrated and is quite different from the three-leg Hubbard model, which can be described as an effective spin- $\frac{1}{2}$  model for large  $U$ . In the large  $U$  limit, this Hubbard model maps to the Heisenberg model, which does not show phase transition. If the coupling strength  $U$  is not strong, due to the presence of charge degrees of freedom, the magnetic frustration may affect the double occupancy and the low-energy properties significantly. Our results of the ED (Ref. 24) and the constrained-path Monte Carlo (CPMC) (Ref. 25) show that as  $t$  increases there is a transition from an antiferromagnetic state to a frustrated state with much smaller spin correlation along the chain. The single particle spectra obtained from the cluster perturbation theory (CPT) (Refs. 26 and 27) exhibit that as  $t$  increases the feature of spin-charge separation is destroyed and there is an insulator-metal transition. The frustrated state corresponds to the appearance of an additional dispersive band near the Fermi surface. The successive order of two transitions depends on the on-site Coulomb interaction.

The paper is organized as follows. The model and the computational method are given in Sec. II. The phase diagrams, spin correlation, and spectral structure are described in Sec. III. Finally the discussion and conclusion are given.

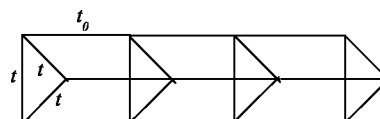


FIG. 1. A quasi-one-dimensional triangular Hubbard model.

## II. MODEL AND COMPUTATIONAL METHOD

The Hubbard model on the lattice in Fig. 1 is defined by

$$H = - \sum_{i=1}^3 \sum_{l,\sigma} t_0 (c_{l,i,\sigma}^\dagger c_{l+1,i,\sigma} + \text{H.c.}) - \sum_{l,\sigma} t (c_{l,1,\sigma}^\dagger c_{l,2,\sigma} + c_{l,1,\sigma}^\dagger c_{l,3,\sigma} + c_{l,2,\sigma}^\dagger c_{l,3,\sigma} + \text{H.c.}) + U \sum_{l,i} n_{l,i,\uparrow} n_{l,i,\downarrow}, \quad (1)$$

here  $c_{l,i,\sigma}^\dagger$  ( $c_{l,i,\sigma}$ ) are the creation (annihilation) operators of electron with spin  $\sigma = \uparrow, \downarrow$  on the  $i$ th site of the  $l$ th cell, respectively.  $n_{l,i,\sigma}$  is the number operator of electron.  $U$  is the on-site Coulomb interaction.  $t$  and  $t_0$  are hopping integrals. In the following discussion, we take  $t_0$  as energy unit.

Using the ED method, we study the ground state phases characterized through the following local spin-spin correlations and spin structure factor:

$$D(l) = - \sum_{i,j} \langle S_{l,i}^z S_{l+1,j}^z \rangle, \quad (2)$$

$$S(q) = \frac{1}{N^2} \sum_{li,mj} e^{iq(l-m)} \langle S_{l,i}^z S_{m,j}^z \rangle, \quad (3)$$

with  $S_{l,i}^z = (n_{l,i,\uparrow} - n_{l,i,\downarrow})/2$ .  $N$  is the number of the sites. From the numerical point of view, ED is limited to small lattice sizes. One must perform a finite size scaling study of the order parameters. The CMPC allows one to extend the numerical calculations to a much larger system size. In the CPMC method,<sup>25</sup> the ground-state wave function is projected from a known initial wave function as importance-sampled branching random walks in an overcomplete space of Slater determinants. The paths of the random walks are constrained so that any Slater determinant generated maintains a positive overlap with the trial wave function.

We use the CPT method to calculate the single-particle spectral function.<sup>26,27</sup> The CPT combines ED of finite clusters with perturbation theory to treat intercluster hopping. The short-distance effects are treated exactly by ED while the long-distance hopping is treated by perturbation theory. Compared with the ED, the CPT can deal with the system with an infinite length. The lattice in Fig. 1 can be divided into identical clusters each with  $N$  sites. Then the system can be treated as a superlattice of clusters, each cluster being composed of ordinary lattice sites. According to the usual Lanczos method,<sup>28</sup> we calculate the cluster Green's function  $G_{li,mj,\sigma}(z)$  which is defined as

$$G_{li,mj,\sigma}(z) = \langle \phi_0 | c_{l,i,\sigma} \frac{1}{z - (H - E_0)} c_{m,j,\sigma}^\dagger | \phi_0 \rangle + \langle \phi_0 | c_{m,j,\sigma}^\dagger \frac{1}{z - (E_0 - H)} c_{l,i,\sigma} | \phi_0 \rangle, \quad (4)$$

where  $z = \omega + i\epsilon$  with  $\epsilon$  being a small positive number.  $|\phi_0\rangle$  and  $E_0$  are the wave function and energy of the ground state of a cluster, respectively. The two terms in  $G_{li,mj,\sigma}$  correspond to electron and hole propagation and are calculated separately. The Green's function  $G(k, z)$  of the full system can be obtained from the cluster Green's function  $G_{li,mj,\sigma}(z)$ .

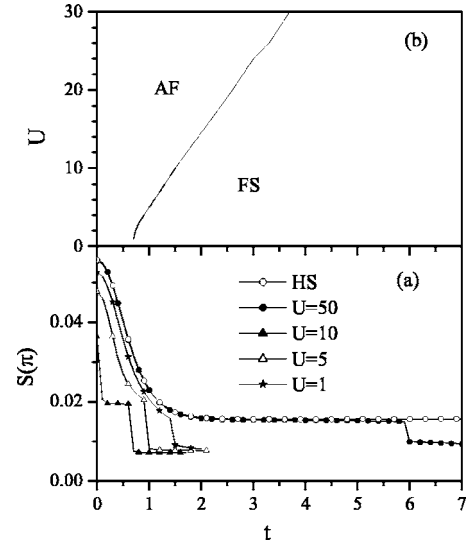


FIG. 2. (a) Spin structure factor  $S(\pi)$  by ED for the cluster  $N = 12$ . HS corresponds to Heisenberg model with exchange interactions  $J=4t^2/U$  and  $J_0=4t_0^2/U$ . (b) The phase diagram showing two ground state phases.

The single-particle spectral function  $A(k, \omega)$  can be obtained from the Green's function  $G(k, z)$

$$A(k, \omega) = - \frac{1}{\pi} \text{Im}[G(k, z)]. \quad (5)$$

The corresponding density of state is defined by

$$N(\omega) = \sum_k A(k, \omega). \quad (6)$$

## III. RESULTS AND DISCUSSION

In the large  $U$  limit, the Hubbard model in Eq. (1) maps to the antiferromagnetic Heisenberg model with exchange interactions  $J_0=4t_0^2/U$  and  $J=4t^2/U$ . In the following discussion, we take  $t_0$  as the energy unit. Figure 2(a) shows the spin structure factor  $S(q)$  at  $q=\pi$  obtained by the ED for a  $N=12$  sites cluster under periodic boundary conditions. The curve HS corresponds to the Heisenberg model with exchange interactions  $J$  and  $J_0$ . It is seen that with increasing  $t$ , the antiferromagnetic correlation decreases due to the magnetic frustration. For  $t < 6.0$ , the result of the Hubbard model for  $U=50$  is in good agreement with the Heisenberg model. However, as the frustration hopping  $t$  increases to a critical value  $t_c=6.0$ , the spin structure factor  $S(\pi)$  drops to a lower stage in the Hubbard model while  $S(\pi)$  is still a constant in the Heisenberg model. This result indicates that in the Hubbard model at  $U=50$  and  $t=t_c$  there is a transition from the antiferromagnetic state (AF) to a frustrated state (FS). Both ground-state phases have the total spin  $S=0$ . However, for the Heisenberg model there is no phase transition. Obviously, for  $t > t_c$  the Hubbard model cannot map to the Heisenberg model. For smaller  $U$ , this transition is also observed at smaller critical value  $t_c$ . The phase diagram is given in Fig. 2(b).

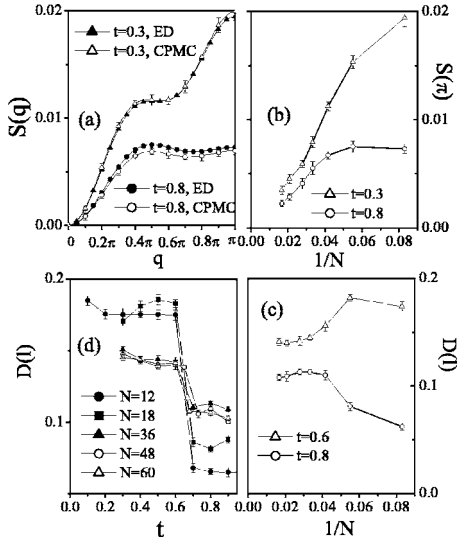


FIG. 3. (a) Spin structure factor  $S(q)$  by ED and CPMC for the cluster  $N=12$ . (b) and (c) The size dependence of  $S(\pi)$  and local spin correlation  $D(l)$ . (d)  $D(l)$  as a function of  $t$ .

It is known that the ED results suffer from finite-size effect. In order to confirm the result in Fig. 2, we perform the CPMC simulation for clusters with size  $N=12, 18, 24, 30, 36, 48$ , and  $60$  clusters. To justify the CPMC program, we compare the results obtained from the ED and the CPMC on the 12-site system. The spin structure  $S(q)$  shown in Fig. 3(a) indicates that the results by two methods are in good agreement in full Brillouin zone. Our experience shows that for small Coulomb interaction, the CPMC method presents us accurate energy and reliable correlation functions even if the trial wave function is a free-electron wave function. For  $U=1$  and  $t=0.3$ , the AF phase is clearly identified with a peak of  $S(q)$  at  $q=\pi$ . When  $t$  increases to  $t>t_c$  (e.g.,  $t=0.8$ ,  $t_c=0.7$  for  $U=1$ ) the spin structure factor shows no evident peak structure. This indicates a transition from the AF phase to the FS phase. From Fig. 3(b) it is found that the spin correlation  $S(\pi)$  in two phases decreases with the cluster sizes and tends to zero in the thermodynamic limit. Hence both phases exhibit no long-range order. Therefore it is more convenient to study the local spin correlation  $D(l)$  defined in Eq. (2). The calculation shows that the translational symmetry is not broken in both phases and  $D(l)$  is independent of unit cell  $l$ . Figure 3(c) shows  $D(l)$  by the two sides ( $t=0.6$  and  $0.8$ ) of the transition point ( $t=0.7$ ) for different clusters with  $N=12, 18, 24, 30, 36, 48$ , and  $60$ . Although  $D(l)$  exhibits a large finite-size effect for small systems one can find that for  $N>30$ ,  $D(l)$  in antiferromagnetic phase ( $t=0.6$ ) and the frustrated phase ( $t=0.8$ ) reaches their stable values in thermodynamic limit. Figure 3(d) shows  $D(l)$  as a function of  $t$  for several clusters with different sizes. The abrupt change near the transition point is very clear for different clusters. The transition point is at about  $t=0.7$  for different clusters. The finite-size effect becomes small for clusters with  $N>30$ . Combining Figs. 3(c) with 3(d) I conclude that to extrapolate to the thermodynamic limit, this phase transition should be still observed.

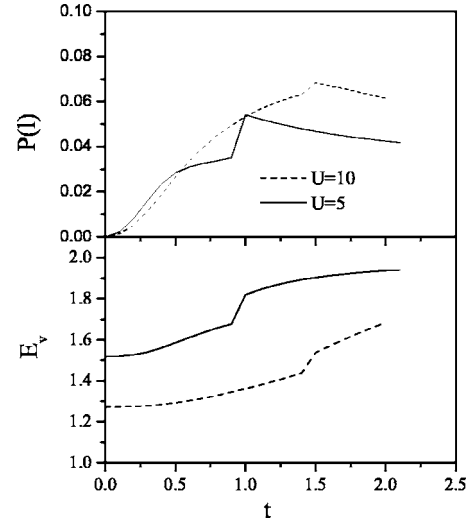


FIG. 4. Local entanglement  $E_v$  and local spin correlation  $P(l)$  as functions of  $t$  for different  $U$ .

The local entanglement is an important quantity to describe quantum phase transition.<sup>29</sup> For the Hubbard model at half-filling, the local entanglement  $E_v$  is

$$E_v = -2w \log_2 w - 2(1/2 - w) \log_2(1/2 - w), \quad (7)$$

here  $w = \langle n_{l,i,\uparrow} n_{l,i,\downarrow} \rangle$  is double occupancy. Figure 4(a) shows the local entanglement  $E_v$  as a function of  $t$  for different  $U$ . With increasing  $t$ , double occupancy  $w$  and the local entanglement  $E_v$  increases. At transition point,  $E_v$  jumps to a higher value. Hence  $E_v$  can be employed to describe the phase transition. In a one-dimensional (1D) extended Hubbard model, the local entanglement either reaches the maximum value or shows singularity at the critical point.<sup>29</sup> Obviously, the behaviour of  $E_v$  in the present case is quite different from the 1D extended Hubbard model. The abrupt change of the local spin correlation function  $D(l)$  can be explained by the behavior of  $E_v$ . Because single occupancy is an essential prerequisite for antiferromagnetic correlation, accompanied by a jump of  $w$  or  $E_v$ , the local spin correlation function  $D(l)$  drops to a lower stage at the critical point.

In order to exhibit the basic physics of the magnetic frustration, we also calculated the local spin correlation  $P(l) = -\langle S_{l,i}^z S_{l,j}^z \rangle$  between different sites of a unit cell. From Fig. 4(b), one can see that with increasing  $t$  this correlation is enhanced. At the critical point  $t=t_c$ , there is a jump to its maximum. This feature can be explained by following scenario. For small  $t$ , when  $t$  increases the effect exchange interaction  $J=4t^2/U$  increases so that the antiferromagnetic correlation  $P(l)$  is enhanced. At  $t=t_c$ , the system transits to a frustrated state (FS) with a maximum  $P(l)$ . As  $t$  increases continuously, the Hubbard model cannot map to the Heisenberg model due to a large double occupancy so that  $P(l)$  decreases. Hence  $P(l)$  can be used to measure the extent of the magnetic frustration.

Now we discuss the possible insulator-metal transition. The Hubbard model in Eq. (1) is metallic in the absence of electron-electron interaction. The three bands are given by

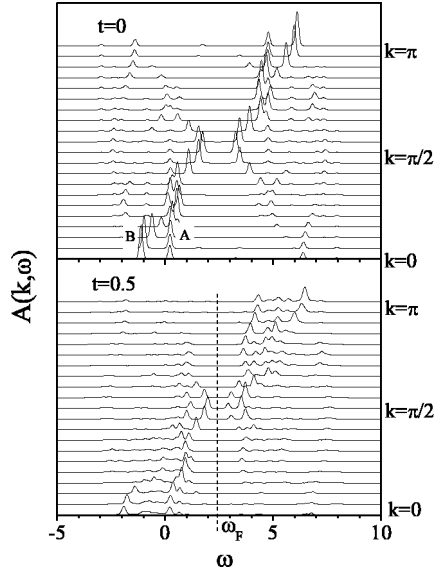


FIG. 5. Spectral function  $A(k, \omega)$  for  $U=5.0$  and  $t=0$  and  $0.5$ , respectively.  $\omega_F$  denotes Fermi level.

$$\epsilon_1(k) = -2t - 2t_0 \cos k, \quad (8)$$

$$\epsilon_{2,3}(k) = t - 2t_0 \cos k. \quad (9)$$

Obviously  $\epsilon_2(k)$  and  $\epsilon_3(k)$  are degenerate. For  $t=0$  and  $U > 0$ , the Hubbard model in Eq. (1) decouples to the 1D Hubbard model and is an antiferromagnetic insulator. Hence it is interesting to judge whether there is a transition from insulator to metal when the frustration hopping  $t$  increases. The charge gap is an important order parameter to discuss this problem.<sup>30</sup> It has been plausibly argued that the charge gap is twice the excitation gap,<sup>31</sup> which can be obtained from the spectral function. Figure 5 shows the single-particle spectral function  $A(k, \omega)$  obtained by the CPT for the system with an infinite length. The Fermi surface is at  $\omega = \omega_F$ . The spectral weights for  $\omega \leq \omega_F$  and  $\omega > \omega_F$  correspond to the photoemission spectra and the inverse photoemission spectra, which is created by removing an electron or a hole from the ground state, respectively. The case for  $t=0$  corresponds to the 1D Hubbard model. To compare the upper panel of Fig. 5 of this article with Fig. 3 of Ref. 26, one can clearly identify the spinon  $A$  and holon  $B$  branches, characteristic of a Luttinger liquid with a charge gap. Other branches corresponding to Fig. 3 of Ref. 26 are also observed clearly. As  $t$  is turned on, the particle-hole symmetry in spectra is destroyed since the structure is not a bipartite lattice. For  $t=0.5$ , spin-charge separation cannot be identified in the spectra while the excitation gap decreases. This result means that the magnetic frustration is not in favor of the Luttinger liquid. As  $t$  increases continuously, the excitation gap may disappear. Figure 6 shows the density of state  $N(\omega)$  for  $U=5$  and different  $t$ . It is found that as  $t$  increases to another critical point  $t_c=0.9$  the gap disappears indicating a transition from insulator to metal. Combining results in Figs. 2 and 6, we find that for small  $t$  the system is an antiferromagnetic insulator (AFI), which turns to an antiferromagnetic metal (AFM) at

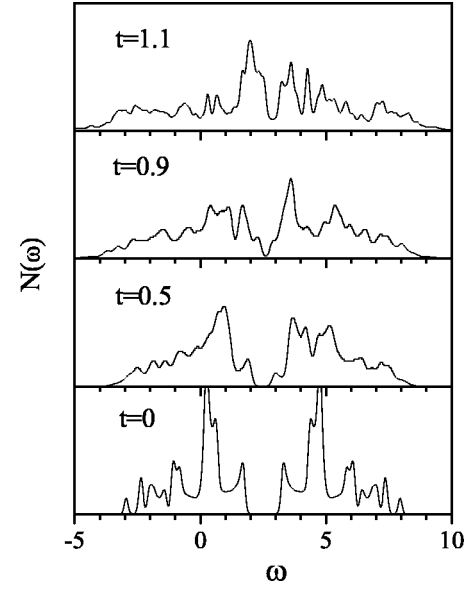


FIG. 6. Density of state (DOS)  $N(\omega)$  for  $U=5$ .

$t_c=0.9$ . Further increasing  $t$ , at  $t=t_c=1.0$  a frustrated metal (FSM) corresponding to the jump of  $E_v$  and  $P(l)$  in Fig. 4 is stabilized.

To confirm the quantitative reliability of the CPT method, I give a comparison between the ED and CPT methods. In their original paper,<sup>26</sup> Sénéchal *et al.* has given a detail comparison between the ED and CPT methods. For the 1D Hubbard model, the quality of the CPT spectrum for cluster  $N=4$  is comparable with that of the ED spectra for cluster  $N=12$ . In the present model, the excitation gap is an important quantity since I use the CPT method to estimate the insulator-metal transition. Figure 7 shows  $N(\omega)$  for  $U=5.0$  and  $t=0.9$  by the ED and CPT methods. The spectral structures by the two methods are similar while the peaks by the ED method are more sharp. Moreover, the CPT predicts that at  $t=0.9$  the gap disappears and there is an insulator-metal transition while the ED does not. Now, I discuss why these differences exist. The ED treats a single cluster with  $N=12$  sites while the CPT treats an infinite system consisting of

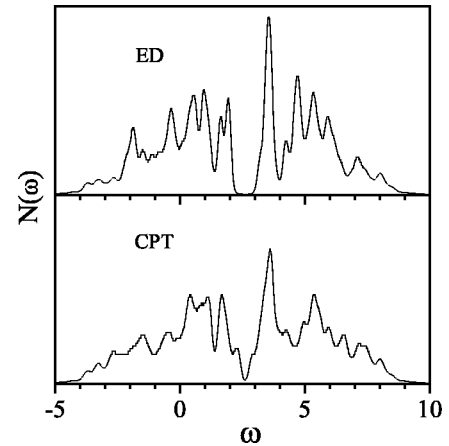


FIG. 7. Density of state  $N(\omega)$  by the ED and the CPT for  $U=5$  and  $t=0.9$ .

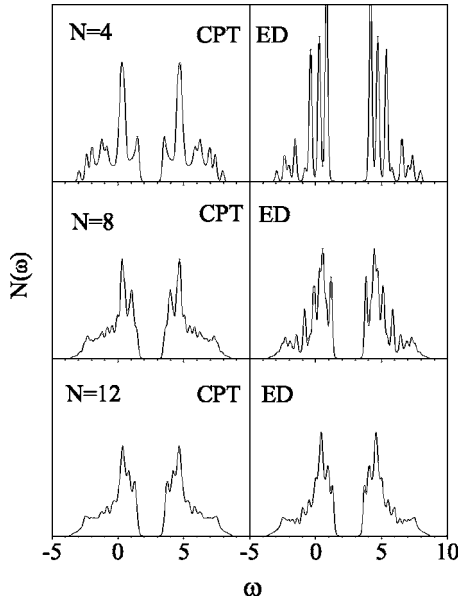


FIG. 8. Density of state  $N(\omega)$  by the ED and the CPT for 1D Hubbard model for  $U=5$  and cluster size  $N=4, 8,$  and  $12$ .

identical clusters each with  $N=12$  sites. As a result, the finite-size effect is large for the ED since the cluster of four unit cells is too small. In order to estimate the finite-size effect of the excitation gap, for the 1D Hubbard model I calculate the quantity  $N(\omega)$  with different lengths  $N$ . The results by the ED and CPT methods are shown in Fig. 8. It is found that with increasing  $N$ , the gap by the ED decreases and shows a large finite-size effect. However, the gap by the CPT for  $N=4$  is comparable with that of the ED for  $N=12$  and shows very small finite-size effect. For small clusters, the gap by the ED is larger than that by the CPT (e.g., in Fig. 7). In the present model, the largest size that can be treated by the ED is  $N=12$  (four unit cells), the precise treatments of the finite-size effects is impossible. Hence, the CPT method is more appropriate to treat the insulator-metal transition in present model.

The successive order of two transitions may be different for different Coulomb interaction  $U$ . Figure 9 shows the spectra for  $U=8$  and different  $t$ . It is found that for small  $t=1.1$  the spectra exhibits a large excitation gap and the system is AFI. As  $t > t_c = 1.3$  [e.g.,  $t=1.4$  in Fig. 9(b)], another branch having a clear dispersion between  $k=0$  to  $\pi/4$  appears near the Fermi level. The system becomes a frustrated insulator (FSI). The presence of this quasiparticle band in the FSI phase corresponds to the jumps of the local entanglement and double occupancy at the critical point  $t_c$  in Fig. 4. In photoemission spectra, the spectral weight near (far from) the Fermi level is created by removing an electron from a doubly (singly) occupied site. Since at the critical point  $t_c$  double occupancy increases abruptly as in Fig. 4, there is the additional spectral weight with low binding energy. This quasiparticle branch is another signature of the FSI phase. Let us discuss it. For  $t=0$ , the model in Eq. (1) decouples to a 1D Hubbard model and the Fermi level is at  $k_F = \pi/2$ . The properties of the system are dominated mainly by the 1D Hubbard model and the spin-charge separation is observed in

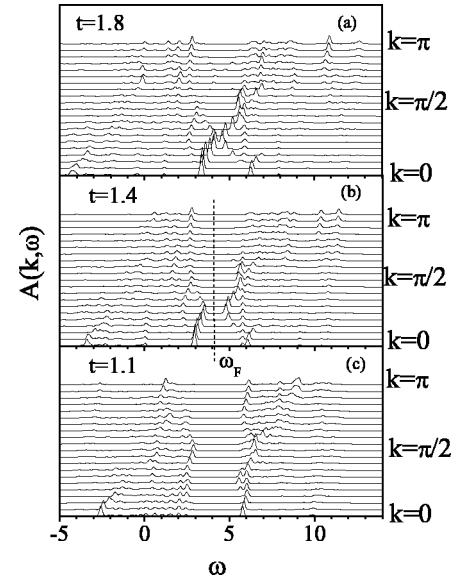


FIG. 9. Spectral function  $A(k, \omega)$  for  $U=8.0$ .

Fig. 5. As  $t$  increases, the interaction between holons and spinons is enhanced and their separation cannot be identified. As  $t$  is large enough, for the noninteracting system, the lower band  $\epsilon_1(k)$  is filled and the higher band  $\epsilon_{2,3}(k)$  is partly filled with the Fermi point  $k_F = \pi/4$  [see Eqs. (8) and (9)]. Figure 9(b) indicates that as  $t$  increases to a critical  $t_c$ , the low-energy quasiparticle band follows the free-particle dispersion  $\omega = \omega_F - 2t_0 \cos k$  between  $k=0$  to  $k_F = \pi/4$ . In the triangular lattice, it was also observed that frustration assists the formation of Fermi quasiparticles by effectively suppressing the antiferromagnetic fluctuations.<sup>15</sup>

As  $t$  increases to another critical point  $t_{c'} = 1.8$ , the gap vanishes in Fig. 9(a) while the low-energy quasiparticle branch near the Fermi level still exists. The system transforms to FSM phase. For small  $U$  (e.g.,  $U=5$ ), this additional branch is also observed in the FSM phase but not shown here. The phase diagram showing four different ground-state phases AFI, AFM, FSI, and FSM is given in Fig. 10. Because the CPT method is adequate at intermediate coupling we just

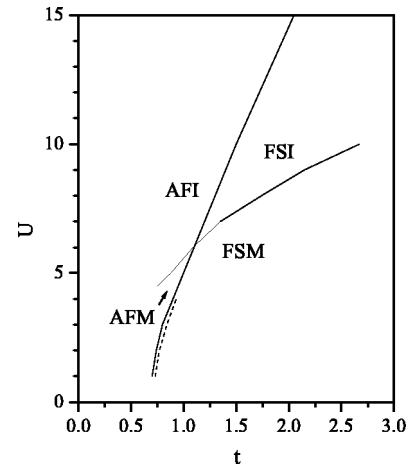


FIG. 10. Phase diagram showing four ground state phases. The dashed line is the extrapolated results from the CPMC.

give the result for  $10 > U > 4$ . It is found that with increasing  $t$  there are two transitions from antiferromagnetic state to frustrated state and from insulator to metal, which successive order depends on  $U$ . The dashed line indicates the extrapolated value of  $t_c$  by the CPMC. Our experience shows that for small Coulomb interaction  $U$ , the CPMC method presents accurate energy and reliable correlation functions even if the trial wave function is a free-electron wave function. But for large  $U$ , the choice of the trial wave function is important to obtain reliable results. Hence I just present the extrapolated results for  $U < 4$  in Fig. 10. In this paper, the CPMC method is just employed to confirm the existence of the critical point  $t_c$  separating the antiferromagnetic and a frustrated state. Most of the results are obtained from the ED and CPT methods and are qualitative.

In summary, we study the magnetic frustration in a quasi-one-dimensional triangular Hubbard model with many-body

methods including ED, CPMC, and CPT. As the frustration hopping  $t$  is small the system exhibits antiferromagnetic correlation. As  $t > t_c$ , there is a transition from an antiferromagnetic state to a frustrated state. This transition is accompanied by a jump of local entanglement and an abrupt change of spin correlation. As  $t > t_{c'}$ , the insulator-metal transition occurs. The successive order of two transitions depends on the coupling strength  $U$ . The calculated spectra indicates that the spin-charge separation is destroyed by  $t$ . The frustrated state corresponds to the appearance of additional dispersion band near the Fermi surface.

#### ACKNOWLEDGMENTS

This work was supported by the National Natural Science Foundation of China under Grant Nos. 10004004 and 10374073, and FANEDD of China under Grant No. 200034.

---

\*Email address: wzwang@whu.edu.cn

- <sup>1</sup>I. S. Hagemann, Q. Huang, X. P. A. Gao, A. P. Ramirez, and R. J. Cava, *Phys. Rev. Lett.* **86**, 894 (2001).
- <sup>2</sup>J. van Lierop and D. H. Ryan, *Phys. Rev. Lett.* **86**, 4390 (2001).
- <sup>3</sup>M. Fiebig, C. Degenhardt, and R. V. Pisarev, *Phys. Rev. Lett.* **88**, 027203 (2002).
- <sup>4</sup>M. Tissier, B. Delamotte, and D. Mouhanna, *Phys. Rev. Lett.* **84**, 5208 (2000).
- <sup>5</sup>R. Schmidt, J. Schulenburg, J. Richter, and D. D. Betts, *Phys. Rev. B* **66**, 224406 (2002).
- <sup>6</sup>S. Burdin, D. R. Grempel, and A. Georges, *Phys. Rev. B* **66**, 045111 (2002).
- <sup>7</sup>B. Canals, *Phys. Rev. B* **65**, 184408 (2002).
- <sup>8</sup>W. Brenig and A. Honecker, *Phys. Rev. B* **65**, 140407(R) (2002).
- <sup>9</sup>V. Elser, *Phys. Rev. Lett.* **62**, 2405 (1989); J. T. Chalker and J. F. G. Eastmond, *Phys. Rev. B* **46**, 14 201 (1992).
- <sup>10</sup>S. Eggert, *Phys. Rev. B* **54**, R9612 (1996).
- <sup>11</sup>N. Lafflorencie and D. Poilblanc, *Phys. Rev. Lett.* **90**, 157202 (2003).
- <sup>12</sup>A. Koga and N. Kawakami, *Phys. Rev. B* **63**, 144432 (2001).
- <sup>13</sup>S. Fujimoto, *Phys. Rev. Lett.* **89**, 226402 (2002).
- <sup>14</sup>S. Fujimoto, *Phys. Rev. B* **67**, 235102 (2003).
- <sup>15</sup>Y. Imai and N. Kawakami, *Phys. Rev. B* **65**, 233103 (2002).
- <sup>16</sup>Y. Imai, N. Kawakami, and H. Tsunetsugu, *Phys. Rev. B* **68**, 195103 (2003).
- <sup>17</sup>S. Daul and R. M. Noack, *Phys. Rev. B* **61**, 1646 (2000).
- <sup>18</sup>L. Capriotti, A. E. Trumper, and S. Sorella, *Phys. Rev. Lett.* **82**, 3899 (1999).
- <sup>19</sup>H. R. Krishnamurthy, C. Jayaprakash, S. Sarker, and W. Wenzel, *Phys. Rev. Lett.* **64**, 950 (1990).
- <sup>20</sup>M. Capone, L. Capriotti, F. Becca, and S. Caprara *Phys. Rev. B* **63**, 085104 (2001).
- <sup>21</sup>S. Daul and D. J. Scalapino, *Phys. Rev. B* **62**, 8658 (2000).
- <sup>22</sup>B. Frischmuth, S. Haas, G. Sierra, and T. M. Rice, *Phys. Rev. B* **55**, R3340 (1997).
- <sup>23</sup>E. H. Lieb and F. Y. Wu, *Phys. Rev. Lett.* **20**, 1445 (1968).
- <sup>24</sup>H. Q. Lin and J. E. Gubernatis, *Comput. Phys.* **7** 400 (1993).
- <sup>25</sup>S. Zhang, J. Carlson, and J. E. Gubernatis, *Phys. Rev. B* **55**, 7464 (1997).
- <sup>26</sup>D. Sénéchal, D. Perez, and M. Pioro-Ladrière, *Phys. Rev. Lett.* **84**, 522 (2000).
- <sup>27</sup>W. Z. Wang, Bambi Hu, and K. L. Yao, *Phys. Rev. B* **66**, 085101 (2002); W. Z. Wang and K. L. Yao, *Europhys. Lett.* **69**, 978 (2005).
- <sup>28</sup>E. Dagotto, *Rev. Mod. Phys.* **66**, 763 (1994).
- <sup>29</sup>S. J. Gu, S. S. Deng, Y. Q. Li, and H. Q. Lin, *Phys. Rev. Lett.* **93**, 086402 (2004).
- <sup>30</sup>M. Imada, A. Fujimori, and Y. Tokura, *Rev. Mod. Phys.* **70**, 1039 (1998).
- <sup>31</sup>N. Shibata, T. Nishino, K. Ueda, and C. Ishii, *Phys. Rev. B* **53**, R8828 (1996).